ACS Infectious Diseases

Article

Anti-SARS-CoV-2 Potential of Artemisinins In Vitro

Ruiyuan Cao, Hengrui Hu, Yufeng Li, Xi Wang, Mingyue Xu, Jia Liu, Huanyu Zhang, Yunzheng Yan, Lei Zhao, Wei Li, Tianhong Zhang, Dian Xiao, xiaojia Guo, Yuexiang Li, Jingjing Yang, Zhihong Hu, Manli Wang, and Wu Zhong

ACS Infect. Dis., **Just Accepted Manuscript** • DOI: 10.1021/acsinfecdis.0c00522 • Publication Date (Web): 31 Jul 2020

is published by the American Chemical Society. 1155 Sixteenth Street N.W., Washington, DC 20036

Anti-SARS-CoV-2 Potential of Artemisinins In Vitro

Ruiyuan Cao[1#], Hengrui Hu[2,3#], Yufeng Li[2,3#], Xi Wang[2], Mingyue Xu[2,3], Jia Liu[2], Huanyu Zhang[2,3], Yunzheng Yan[1], Lei Zhao[1], Wei Li[1], Tianhong Zhang[1,4], Dian Xiao[1], Xiaojia Guo[1], Yuexiang Li[1], Jingjing Yang[1], Zhihong Hu[2*], Manli Wang[2*], Wu Zhong[1*]

[1]National Engineering Research Center for the Emergency Drug, Beijing Institute of Pharmacology and Toxicology, Beijing 100850, China; [2]State Key Laboratory of Virology, Wuhan Institute of Virology, Center for Biosafety Mega-Science, Chinese Academy of Sciences, Wuhan 430071, P. R. China; [3]University of the Chinese Academy of Sciences, Beijing 100049, P. R. China; [4]Guoke Excellence (Beijing) Medicine Technology Research Co., Ltd., Beijing 100176, P. R. China

#These authors contributed equally:

Ruiyuan Cao[1#], Hengrui Hu[2, 3#], Yufeng Li[2, 3#]

*Corresponding authors:

Prof., Dr. Wu Zhong; Mailing address: National Engineering Research Center for the Emergency Drug, Beijing Institute of Pharmacology and Toxicology, Beijing 100850, P. R. China. Tel: 86-10-66932624. E-mail: zhongwu@bmi.ac.cn

Prof., Dr. Manli Wang; Mailing address: Wuhan Institute of Virology, Center for Biosafety Mega-Science, Chinese Academy of Sciences, Wuhan 430071, P. R. China. Tel/Fax: 86-27-87197340. E-mail: wangml@wh.iov.cn

Prof., Dr. Zhihong Hu; Mailing address: Wuhan Institute of Virology, Center for Biosafety Mega-Science, Chinese Academy of Sciences, Wuhan 430071, P. R. China. Tel/Fax: 86-27-87197180. E-mail: huzh@wh.iov.cn

Abstract

The discovery of novel drug candidates with anti-severe acute respiratory coronavirus 2 (SARS-CoV-2) potential is critical for the control of the global COVID-19 pandemic. Artemisinin, an old antimalarial drug derived from Chinese herbs, has saved millions of lives. Artemisinins are a cluster of artemisinin-related drugs developed for the treatment of malaria and have been reported to have multiple pharmacological activities, including anticancer, antiviral, and immune modulation. Considering the reported broad-spectrum antiviral potential of artemisinins, researchers are interested in whether they could be used to combat COVID-19. We systematically evaluated the anti-SARS-CoV-2 activities of nine artemisinin-related compounds *in vitro* and carried out a time-of-drug-addition assay to explore their antiviral mode of action. Finally, a pharmacokinetic prediction model was established to predict the therapeutic potential of selected compounds against COVID-19. Arteannuin B showed the highest anti-SARS-CoV-2 potential with an EC_{50} of 10.28 ± 1.12 μM. Artesunate and dihydroartemisinin showed similar EC_{50} values of 12.98 ± 5.30 μM and 13.31 ± 1.24 μM, respectively, which could be clinically achieved in plasma after intravenous administration. Interestingly, although an EC_{50} of 23.17 ± 3.22 μM was not prominent among the tested compounds, lumefantrine showed therapeutic promise due to high plasma and lung drug concentrations after multiple dosing. Further mode of action analysis revealed that arteannuin B and lumefantrine acted at the post-entry step of SARS-CoV-2 infection. This

research highlights the anti-SARS-CoV-2 potential of artemisinins and provides leading candidates for anti-SARS-CoV-2 drug research and development.

Key words

Artemisinin, SARS-CoV-2, COVID-19, Antiviral drug, Drug repurposing

The COVID-19 pandemic caused by severe acute respiratory coronavirus 2 (SARS-CoV-2) has taken a heavy toll on public health and the global economy. As of July 18, 2020, 13.9 million confirmed cases including 593,087 deaths have been reported worldwide since the pathogen was first identified in January 2020.[1, 2] Unfortunately, there are currently no specific and effective antiviral drugs available to treat a large number of infected patients. Chloroquine, hydroxychloroquine, remdesivir, and lopinavir/ritonavir were highlighted as repurposed drugs to treat COVID-19. However, according to the COVID-19 Treatment Guidelines released by the NIH in April 21, 2020, there are insufficient clinical data to recommend either for or against the use of chloroquine, hydroxychloroquine, and remdesivir for the treatment of COVID-19, and the use of lopinavir/ritonavir or other HIV protease inhibitors was no more recommended.[3] Although a series of Food and Drug Administration (FDA)-approved drugs that are capable of inhibiting SARS-CoV-2 *in vitro* were reported, the discovery of more drug candidates with anti-SARS-CoV-2 potential is urgently needed to fuel antiviral drug research for COVID-19.

Previously, we reported that chloroquine, a decades-old antimalarial drug with immune-modulation activities, and its derivative hydroxychloroquine could efficiently inhibit SARS-CoV-2 *in vitro*.[4, 5] This raises an interesting question of whether other antimalarial drugs also have anti-SARS-CoV-2 potential.[6-8] Artemisinins comprise another series of well-known antimalarials with immunemodulatory activities. Among the reported artemisinins, artemisinin, dihydroartemisinin, artemether-lumefantrine, artesunate, arteether, and artemisone are approved drugs derived from artemisinin.[9-11] Arteannuin B and artemisinic acid are artemisinin derivatives reported to have therapeutic efficacy against malaria *in vivo*.[12, 13] Previous studies have reported the broad-spectrum antiviral potential of artemisinins. For example, artesunate effectively inhibits a wide range of DNA and RNA viruses, including human cytomegalovirus (HCMV), human herpes simplex virus (HSV), hepatitis B virus (HBV), hepatitis C virus (HCV), human immunodeficiency virus (HIV), and polyomavirus BK.[14] Clinical trials focusing on the antiviral efficacy of artesunate suggested that it shows promise for the treatment of patients with HCMV and HSV-2 infection.[15, 16] Dihydroartemisinin also showed inhibitory effects on viruses such as HCMV and Zika virus.[17, 18] In addition, artemisone was proven to be a potent inhibitor of HCMV and had synergistic antiviral activity in combination with other approved and experimental anti-HCMV agents.[19, 20] Considering the broad-spectrum antiviral effects of artemisinins, it is necessary to systematically explore the anti-SARS-CoV-2 potential of artemisinins, which consists of multiple FDA-approved drugs and drug candidates at the late stage of pharmacological development, and predict their therapeutic efficacy based on a physiologically based pharmacokinetic (PBPK) model.

Results

Artemisinins Inhibit SARS-CoV-2 In Vitro

In this study, nine artemisinins (Figure 1) were chosen to test their anti-SARS-CoV-2 potential using African green monkey kidney Vero E6 cells. Cytotoxicity assays were carried out before the antiviral assay to determine the cytotoxicity of the selected compounds, and viral RNA copies in the supernatants were determined by quantitative real-time PCR (qRT-PCR) to determine the antiviral effects of the compounds. The results showed that the half-cytotoxic concentrations (CC_{50}) of arteether, artemether, artemisic acid, artemisinin, and artemisone were greater than 200 μM. However, the half-maximal effective concentrations (EC_{50}) were 31.86 ± 4.72 μM, 73.80 ± 26.91 μM, >100 μM, 64.45 ± 2.58 μM, and 49.64 ± 1.85 μM, respectively for these compounds, indicating sub-optimal selective indexes (SIs) (Figure 2). The EC_{50} of dihydroartemisinin was 13.31 ± 1.24 μM and the SI was 2.38 ± 0.22. Notably, artesunate, which was reported to have broad-spectrum antiviral potential against multiple medical viruses, showed an ideal EC_{50} value of 12.98 ± 5.30 μM against SARS-CoV-2 virus, and its SI was 5.10 ± 2.08. For arteannuin B, the EC_{50} against SARS-CoV-2 was 10.28 ± 1.12 μM, and a CC_{50} of 71.13 ± 2.50 μM led to an optimal SI of 7.00 ± 0.76 among all artemisinins tested. Interestingly, for lumefantrine, another antimalarial drug which is structurally distinct from artemisinins and is a major component of the compound preparation 'coartem', the EC_{50} against SARS-CoV-2 was 23.17 ± 3.22 μM, and its SI was greater than 4.40 ± 0.61.

Artemisinins Reduce the Production of SARS-CoV-2 Protein

To provide more direct evidence of the inhibitory effect of artemisinins, an immunofluorescence assay (IFA) was performed. SARS-CoV-2 nucleoprotein (NP) was stained with a specific antibody and detected with a secondary antibody with a fluorescence label. Inhibition of fluorescence was observed in a dose-dependent manner for several artemisinins, as shown in Figure 3. The expression of viral NP protein was completely inhibited when arteannuin B was added at 25 μM, and most viral NP protein was inhibited when artesunate, dihydroartemisinin, and lumefantrine were added at 25 μM, 25 μM, and 100 μM, respectively. The IFA results were consistent with the viral yield based on qRT-PCR analysis (Figure 2).

Arteannuin B and Lumefantrine Block SARS-CoV-2 Infection at the Post-entry Level

To explore the antiviral mechanism of the selected drugs, the time-of-drug-addition assays were performed for arteannuin B and lumefantrine, which were selected as representatives for different core structure types (Figure 1). Cells were treated with 25 μM of arteannuin B or 100 μM of lumefantrine at different steps of infection (full-time, entry, and post-entry), which was followed by qRT-PCR, IFA, and western blot assays to determine the overall virus replication efficiency. For arteannuin B, addition of the compounds at the entry step failed to inhibit the extracellular viral RNA production and intracellular viral protein expression, but the significant inhibition of viral RNA (Figure 4A) and viral protein (Figure 4B-C) was observed when the drug was added at the post-entry step. Similarly, lumefantrine showed inhibitory effects when added during the full-time infection process or post-entry stage, but not during virus entry (Figure 4A, 4D-E). These data revealed that arteannuin B and lumefantrine might function at a similar stage by interfering with the intracellular events of the SARS-CoV-2 infection cycle, which requires further investigation.

Physiologically Based Pharmacokinetic Modeling and In Vitro to In Vivo Extrapolation (IVIVE) for Lumefantrine

The IVIVE could be estimated for most artemisinins due to the known pharmacokinetic profiles; however, there are limited data on the pharmacokinetics of lumefantrine. We thus carried out PBPK modeling and IVIVE for lumefantrine. Due to the low hepatic clearance and negligible renal excretion of lumefantrine, the prolonged half-life of up to 6 days in healthy volunteers led to a cumulative effect after multi-dose administration.[21] As shown in Figure 5, after six oral doses of 480 mg over 3 days, the EC_{50} of lumefantrine was reached both in plasma and in the lungs. These results suggest the potential of lumefantrine as a potential anti-SARS-CoV-2 agent.

Discussion

During the fight against the COVID-19 pandemic, drug repurposing has been highlighted, as the known safety and pharmacokinetic profiles of repurposed drugs indicate that they are more likely to be applied in a timely manner compared to new drugs. Antimalarial drugs such as chloroquine, quinines, and artemisinins have long histories of clinical application and have been reported to have broad-spectrum antiviral potential in recent years. Chloroquine is effective against influenza virus, dengue virus, and SARS-CoV-2 *in vitro* and has recently been proven to be clinically effective against HCV.[22] Quinines were reported to have antiviral effects against dengue virus and HSV-1.[23, 24] Artesunate is a structural derivative of artemisinin characterized by its broad-spectrum antiviral potential against DNA and RNA viruses.[14] In this study, we systematically evaluated the antiviral potential of artemisinins against SARS-CoV-2 *in vitro* and discovered that artesunate could inhibit SARS-CoV-2 replication in a dose-dependent manner. Arteannuin B is another artemisinin derivative that had an ideal EC_{50} value, suggesting its anti-SARS-CoV-2 effect *in vitro*. Interestingly, we found that the antimalarial drug lumefantrine, which is structurally distant from artemisinins and is a major component of an approved drug coartem, could inhibit SARS-CoV-2 *in vitro* with an EC_{50} of 23.17 ± 3.22 μM.

For the emergency use of repurposed drugs, the pharmacokinetic profile is an important reference for estimating clinical efficacy. The Cmax of artesunate was

42 μM following a single intravenous injection dose of 120 mg, which is greater than the EC_{50} of 13.31 ± 1.24 μM (the *in vivo* metabolite of artesunate was dihydroartemisinin) against SARS-CoV-2, indicating that artesunate is a potential countermeasure against COVID-19.[25] Coartem is a pharmaceutical compound preparation composed of artemether-lumefantrine (20 mg artemether and 120 mg lumefantrine per tablet). The Cmax of artemether was found to be low (0.28 μM); however, the Cmax of lumefantrine was much higher. Moreover, the plasma half-life of lumefantrine was determined to be 119 h, and the long half-life caused drug accumulation, which might lead to enhanced plasma and tissue drug concentrations.[26] Indeed, based on the PBPK model of lumefantrine, the plasma and the lung concentrations could exceed 23.17 μM (12.26 μg/mL) after six oral doses of 480 mg over 3 days, which would exceed its EC_{50} value against SARS-CoV-2. Arteannuin B showed anti-SARS-CoV-2 potential with an EC_{50} of 10.28 ± 1.12 μM, and its unique core structure provided information for the future optimization of artemisinins as anti-SARS-CoV-2 agents.

Artemisinins, especially artesunate and its active metabolite dihydroartemisinin, have been shown to have antiviral potential in the present and previous studies. Accumulating studies have suggested that artesunate is likely to impair viral infection by modulating host cell metabolic pathways. In particular, the anti-HCMV efficacy of artesunate is associated with the PI3-K/Akt/p70S6K signaling pathway. Artesunate was also found to interact directly or indirectly with cellular DNA-binding factors such as NF-κB or Sp1, leading to the inhibition of viral replication.[27, 28] For coartem and arteannuin B, although there are some studies on their antiviral efficacy, our research has demonstrated their promising therapeutic advantages for the treatment of SARS-CoV-2 infection *in vitro*. Notably, synergistic effects of artemisinins and conventional antiviral drugs were observed in antiviral research, including HCMV, HBV, and bovine viral diarrhea virus.[29-31] Facing the global outbreak of SARS-CoV-2, the combination of artemisinins and other antiviral drugs with different mechanisms, such as remdesivir and favipiravir, might be a promising clinical option.

In summary, we systematically explored the antiviral activities of artemisinins against SARS-CoV-2 *in vitro*. Artesunate, arteannuin B, and lumefantrine showed promise as anti-SARS-CoV-2 agents *in vitro*. Combined with the safety and potential immunoregulatory activities of artemisinins, we believe that artemisinin might represent a potential medical countermeasure against COVID-19.

Methods

Cells and Virus

Vero E6 cells (ATCC, no. 1586) were grown and maintained in minimum Eagle's medium (Gibco Invitrogen) supplemented with 10% fetal bovine serum

(Gibco Invitrogen) at 37°C in 5% CO_2. The SARS-CoV-2 strain (nCoV-2019BetaCoV/Wuhan/WIV04/2019) was propagated, stored, and titrated as previously described.[32, 33] All studies on infectious viruses were performed in a biosafety level-3 (BLS-3) laboratory.

Cytotoxicity and Antiviral Assays

Cytotoxicity was evaluated in Vero E6 cells using a cell counting kit-8 (CCK8) (Beyotime, China) according to the manufacturer's instructions. For the antiviral assay, 4.8×10^6 Vero E6 cells were seeded onto 48-well cell-culture Petri dishes and grown overnight. After pretreatment with a gradient of diluted experimental compounds for 1 h at 37°C, cells were infected with virus at an MOI of 0.01 for 1 h. After incubation, the inoculum was removed, cells were washed with PBS, and culture vessels were replenished with fresh drug-containing medium. At 24 h post-infection, total RNA was extracted from the supernatant and qRT-PCR was performed to quantify the virus yield as described previously.[4]

Immunofluorescence Assay

The IFA was performed according to the previous method with modifications.[4] Briefly, Vero E6 cells were inoculated in 48-well cell-culture Petri dishes and grown overnight. After pretreatment with a gradient of diluted experimental compounds for 1 h at 37°C, cells were infected with virus at an MOI of 0.01 for

1 h. After incubation, the inoculum was removed, cells were washed with PBS, and culture vessels were replenished with fresh drug-containing medium. At 24 h post-infection, cells were washed with PBS and fixed with 4% (w/v) paraformaldehyde and permeabilized with 0.2% (v/v, in PBS) triton X-100. After blocking with 5% (m/v, in PBS) bovine serum albumin at 37°C for 1h, the cells were further incubated with the primary antibody, rabbit serum against NP (anti-NP antibody, 1:1000), followed by incubation with the secondary antibody, Alexa 488-labeled goat anti-rabbit (1:500; Abcam). The nucleus was stained with Hoechst 33258 (Beyotime, China). Immunofluorescence images were obtained using a fluorescence microscope.

Time-of-Drug-Addition Assay

The time-of-drug-addition assay was performed according to a previous description.[4] Briefly, Vero E6 cells were seeded at 1 × 10^5 cells/well and incubated overnight. Twenty-five micromolar arteannuin, 100 μM lumefantrine, or DMSO was added at the indicated time points. At 16 h.p.i., the viral NP protein in the infected cells was detected by IFA and western blotting. IFA was performed as described previously herein. Rabbit serum against NP and horseradish peroxidase (HRP)-conjugated goat anti-rabbit IgG (1:5000; Proteintech, China) were used as primary and secondary antibodies, respectively, for western blotting.

Physiologically Based Pharmacokinetic Modeling and Simulations

PBPK simulations were performed using the Simcyp® simulator (Version 18 Release 2, Simcyp Limited, Sheffield, UK) run on a Lenovo computer platform with an Intel® Core i5 processor. All simulations were carried out using the virtual clinical trials composed by the pre-validated in-built 'Healthy Volunteer' population groups. The parameters and methods of PBPK modeling and simulations are available in the supporting information.

Data and Statistical Analysis

The data and statistical analysis in this study complied with the recommendations on experimental design and analysis in pharmacology. The data are presented as the mean ± SEM. Statistical analyses between two groups were performed using the unpaired Student's t-test. Differences among groups were assessed by one-way analysis of variance with the Bonferroni post hoc test. In all cases, a value of $P < 0.05$ was considered statistically significant.

Materials

Artemisinin (CAS No. 63968-64-9), artemether (CAS No. 71963-77-4), artesunate (CAS No. 88495-63-0), dihydroartemisinin (CAS No. 71939-50-9), artemisinic acid (CAS No. 80286-58-4), arteether (CAS No. 75887-54-6), and lumefantrine (CAS No. 82186-77-4) were purchased from Selleck. Arteannuin B (CAS No. 50906-56-4) and artemisone (CAS No. 255730-18-8) were purchased from MedChemExpress. All compounds were dissolved in DMSO for subsequent experiments.

Authors Contributions WZ, MW, ZH, and RC conceived the overall study and designed the experiments. HH, YL, XW, MX, JL, HZ, YY, LZ, WL, TZ, DX, XG, YL, and JY performed most of the biological and functional experiments and analyzed the data. RC, MW, and ZH wrote and edited the manuscript. All authors have made important comments regarding the manuscript.

Conflict of interest The authors declare no conflicts of interest.

Supporting Information Available The detailed methods and results of PBPK modeling are available in the supporting information. This information is available free of charge on the ACS Publications website.

Acknowledgements This research was supported by grants from the National Science and Technology Major Projects (2018ZX09711003) and the National Key Research and Development Project (2020YFC0841700). We thank Jia Wu, Hao Tang, and Jun Liu from BSL-3 Laboratory, from the Core Faculty of Wuhan Institute of Virology for their critical support.

References

1. WHO. (2020). Coronavirus disease (COVID-2019) situation reports - 180. Retrieved from https://www.who.int/docs/default-source/coronaviruse/situation-reports/20200718-covid-19-sitrep-180.pdf?sfvrsn=39b31718_2, accessed on July 21th, 2020

2. Zhu, N., Zhang, D., Wang, W., Li, X., Yang, B., Song, J., Zhao, X., Huang, B., Shi, W., Lu, R., Niu, P., Zhan, F., Ma, X., Wang, D., Xu, W., Wu, G., Gao, G. F., Tan, W., and China Novel Coronavirus Investigating and Research Team. (2020). A Novel Coronavirus from Patients with Pneumonia in China, 2019. *N. Engl. J. Med.* 382, 727-733. DOI:

10.1056/NEJMoa2001017

3. National Institutes of Health.(2020). Coronavirus Disease 2019 (2019-nCoV) Treatment Guidelines. Retrieved from https://www.covid19treatmentguidelines.nih.gov/antiviral-therapy/, accessed on June 29th, 2020

4. Wang, M., Cao, R., Zhang, L., Yang, X., Liu, J., Xu, M., Shi, Z., Hu, Z., Zhong, W., and Xiao, G. (2020). Remdesivir and chloroquine effectively inhibit the recently emerged novel coronavirus (2019-nCoV) in vitro. *Cell Res.* 30, 269-271. DOI: 10.1038/s41422-020-0282-0

5. Hedya, S. A., Safar, M. M., and Bahgat, A. K. (2019). Hydroxychloroquine antiparkinsonian potential: Nurr1 modulation versus autophagy inhibition. *Behav. Brain. Res.* 365, 82-88. DOI: 10.1016/j.bbr.2019.02.033

6. Cheong, D. H. J., Tan, D. W. S., Wong, F. W. S., and Tran, T. (2020). Anti-malarial drug, artemisinin and its derivatives for the treatment of respiratory diseases. *Pharmacol. Res. 158*, 104901. DOI: 10.1016/j.phrs.2020.104901

7. Uzun, T., and Toptas, O. (2020). Artesunate: could be an alternative drug to chloroquine in COVID-19 treatment? *Chin. Med.* 15, 54. DOI: 10.1186/s13020-020-00336-8

8. Ho, W. E., Peh, H. Y., Chan, T. K., and Wong, W. S. (2014). Artemisinins: pharmacological actions beyond anti-malarial. *Pharmacol. Ther.* 142, 126-139. DOI: 10.1016/j.pharmthera.2013.12.001

9. Afolabi, B. B., and Okoromah, C. N. (2004). Intramuscular arteether for treating severe malaria. *Cochrane Database Syst. Rev.* 2004, CD004391. DOI: 10.1002/14651858.CD004391.pub2

10. Sinclair, D., Zani, B., Donegan, S., Olliaro, P., and Garner, P. (2009). Artemisinin-based combination therapy for treating uncomplicated malaria. *Cochrane Database Syst. Rev.* 2009, CD007483. DOI: 10.1002/14651858.CD007483.pub2

11. Waknine-Grinberg, J. H., Hunt, N., Bentura-Marciano, A., McQuillan, J. A., Chan, H. W., Chan, W. C., Barenholz, Y., Haynes, R. K., and Golenser, J. (2010). Artemisone effective against murine cerebral malaria. *Malar. J.* 9, 227. DOI: 10.1186/1475-2875-9-227

12. Cai, T. Y., Zhang, Y. R., Ji, J. B., and Xing, J. (2017). Investigation of the component in Artemisia annua L. leading to enhanced antiplasmodial potency of artemisinin via regulation of its metabolism. *J. Ethnopharmacol.* 207, 86-91. DOI: 10.1016/j.jep.2017.06.025

13. Lee, J., Kim, M. H., Lee, J. H., Jung, E., Yoo, E. S., and Park, D. (2012). Artemisinic acid is a regulator of adipocyte differentiation and /EBP delta expression. *J. Cell Biochem.* 113, 2488-2499. DOI: 10.1002/jcb.24124

14. Efferth, T., Romero, M. R., Wolf, D. G., Stamminger, T., Marin, J. J., and Marschall, M. (2008). The antiviral activities of artemisinin and artesunate. *Clin. Infect. Dis.* 47, 804-811. DOI: 10.1086/591195

15. Raffetin, A., Bruneel, F., Roussel, C., Thellier, M., Buffet, P., Caumes, E., and Jaureguiberry, S. (2018). Use of artesunate in non-malarial indications. *Med. Mal. Infect.* 48, 238-249. DOI: 10.1016/j.medmal.2018.01.004

16. Shapira, M. Y., Resnick, I. B., Chou, S., Neumann, A. U., Lurain, N. S., Stamminger, T., Caplan, O., Saleh, N., Efferth, T., Marschall, M., and Wolf, D. G. (2008). Artesunate as a potent antiviral agent in a patient with late drug-resistant cytomegalovirus infection after hematopoietic stem cell transplantation. *Clin. Infect. Dis.* 46, 1455-1457. DOI: 10.1086/587106

17. Flobinus, A., Taudon, N., Desbordes, M., Labrosse, B., Simon, F., Mazeron, M. C., and Schnepf, N. (2014). Stability and antiviral activity against human cytomegalovirus of artemisinin derivatives. *J. Antimicrob. Chemother.* 69, 34-40. DOI: 10.1093/jac/dkt346

18. Han, Y., Pham, H. T., Xu, H., Quan, Y., and Mesplede, T. (2019). Antimalarial drugs and their metabolites are potent Zika virus inhibitors. *J. Med. Virol.* 91, 1182-1190. DOI: 10.1002/jmv.25440

19. Oiknine-Djian, E., Bar-On, S., Laskov, I., Lantsberg, D., Haynes, R. K., Panet, A., and Wolf, D. G. (2019). Artemisone demonstrates synergistic antiviral activity in combination with approved and experimental drugs active against human cytomegalovirus. *Antiviral Res.* 172, 104639. DOI: 10.1016/j.antiviral.2019.104639

20. Oiknine-Djian, E., Weisblum, Y., Panet, A., Wong, H. N., Haynes, R. K., and Wolf, D. G. (2018). The Artemisinin Derivative Artemisone Is a Potent Inhibitor of Human Cytomegalovirus Replication. *Antimicrob. Agents Chemother.* 62, e00288-18. DOI: 10.1128/AAC.00288-18

21. Borrmann, S., Sallas, W. M., Machevo, S., González, R., Björkman, A., Mårtensson, A., Hamel, M., Juma, E., Peshu, J., Ogutu, B., Djimdé, A., D'Alessandro, U., Marrast, A. C., Lefèvre, G., and Kern, S. E. (2010). The effect of food consumption on lumefantrine bioavailability in African children receiving artemether-lumefantrine crushed or dispersible tablets (Coartem) for acute uncomplicated Plasmodium falciparum malaria. *Trop. Med. Int. Health* 15, 434-441. DOI: 10.1111/j.1365-3156.2010.02477.x

22. Peymani, P., Yeganeh, B., Sabour, S., Geramizadeh, B., Fattahi, M. R., Keyvani, H., Azarpira, N., Coombs, K. M., Ghavami, S., and Lankarani, K. B. (2016). New use of an old drug: chloroquine reduces viral and ALT levels in HCV non-responders (a randomized, triple-blind, placebo-controlled pilot trial). *Can. J. Physiol. Pharmacol.* 94, 613-9. DOI: 10.1139/cjpp-2015-0507

23. A. Baroni, I. Paoletti, E. Ruocco, F. Ayala, F. Corrado, R. Wolf, M.A. Tufano,

and G. Donnarumma. (2007). Antiviral effects of quinine sulfate on HSV-1 HaCat cells infected: analysis of the molecular mechanisms involved. *J. Dermatol. Sci.* 47, 253-255. DOI: 10.1016/j.jdermsci.2007.05.009

24. Malakar, S., Sreelatha, L., Dechtawewat, T., Noisakran, S., Yenchitsomanus, P. T., Chu, J. J. H., and Limjindaporn, T. (2018). Drug repurposing of quinine as antiviral against dengue virus infection. *Virus Res.* 255, 171-178. DOI: 10.1016/j.virusres.2018.07.018

25. Ilett, K. F., Batty, K. T., Powell, S. M., Binh, T. Q., Thu, I., Phuong, H. L., Hung, N. C., and Davis, T. M. (2002). The pharmacokinetic properties of intramuscular artesunate and rectal dihydroartemisinin in uncomplicated falciparum malaria. *Br. J. Clin. Pharmacol.* 53, 23-30. DOI: 10.1046/j.0306-5251.2001.01519.x

26. FDA.(2020). *COARTEM® (artemether and lumefantrine) tablets, for oral use*. Retrieved from https://www.accessdata.fda.gov/drugsatfda_docs/label/2019/022268s021lbl.pdf, accessed on June 18th, 2020

27. Eickhoff, J., Hanke, M., Stein-Gerlach, M., Kiang, T. P., Herzberger, K., Habenberger, P., Müller, S., Klebl, B., Marschall, M., Stamminger, T., and Cotten, M. (2004). RICK activates a NF-kappaB-dependent anti-human cytomegalovirus response. *J. Biol. Chem.* 279, 9642-9652. DOI: 10.1074/jbc.M312893200

28. Efferth, T., Marschall, M., Wang, X., Huong, S. M., Hauber, I., Olbrich, A., Kronschnabl, M., Stamminger, T., and Huang, E. S. (2002). Antiviral activity of artesunate towards wild-type, recombinant, and ganciclovir-resistant human cytomegaloviruses. *J. Mol. Med. (Berl)* 80, 233-242. DOI: 10.1007/s00109-001-0300-8

29. Kaptein, S. J., Efferth, T., Leis, M., Rechter, S., Auerochs, S., Kalmer, M., Bruggeman, C. A., Vink, C., Stamminger, T., and Marschall, M. (2006). The anti-malaria drug artesunate inhibits replication of cytomegalovirus in vitro and in vivo. *Antiviral Res.* 69, 60-69. DOI: 10.1016/j.antiviral.2005.10.003

30. Romero, M. R., Efferth, T., Serrano, M. A., Castaño, B., Macias, R. I. R., Briz, O., and Marin, J. J. G. (2005). Effect of artemisinin/artesunate as inhibitors of hepatitis B virus production in an “in vitro” replicative system. *Antiviral Res.* 68, 75-83. DOI: 10.1016/j.antiviral.2005.07.005

31. Romero, M. R., Serrano, M. A., Vallejo, M., Efferth, T., Alvarez, M., and Marin, J. J. (2006). Antiviral effect of artemisinin from Artemisia annua against a model member of the Flaviviridae family, the bovine viral diarrhoea virus (BVDV). *Planta Med.* 72, 1169-1174. DOI: 10.1055/s-2006-947198

32. Huang, C., Wang, Y., Li, X., Ren, L., Zhao, J., Hu, Y., Zhang, L., Fan, G.,

Xu, J., Gu, X., Cheng, Z., Yu, T., Xia, J., Wei, Y., Wu, W., Xie, X., Yin, W., Li, H., Liu, M., Xiao, Y., Gao, H., Guo, L., Xie, J., Wang, G., Jiang, R., Gao, Z., Jin, Q., Wang, J., and Cao, B. (2020). Clinical features of patients infected with 2019 novel coronavirus in Wuhan, China. *The Lancet* 395, 497-506. DOI: 10.1016/s0140-6736(20)30183-5

33. Zhou, P., Yang, X. L., Wang, X. G., Hu, B., Zhang, L., Zhang, W., Si, H. R., Zhu, Y., Li, B., Huang, C. L., Chen, H. D., Chen, J., Luo, Y., Guo, H., Jiang, R. D., Liu, M. Q., Chen, Y., Shen, X. R., Wang, X., Zheng, X. S., Zhao, K., Chen, Q. J., Deng, F., Liu, L. L., Yan, B., Zhan, F. X., Wang, Y. Y., Xiao, G. F., and Shi, Z. L. (2020). A pneumonia outbreak associated with a new coronavirus of probable bat origin. *Nature* 579, 270-273. DOI: 10.1038/s41586-020-2012-7

Figure legends

Figure 1. Structure and approval status of selected artemisinins. Green, approved stage; yellow, drugs in pre-clinical stage.

Figure 2. Anti-SARS-CoV-2 profile of selected artemisinins. Vero E6 cells were infected with SARS-CoV-2 at an MOI of 0.01 for treatment with different doses of the indicated antivirals for 24 h. The viral yield in the cell supernatant was then quantified by qRT-PCR. The cytotoxicity of these drugs against Vero E6 cells was measured by performing CCK-8 assays. The red circles and lines indicate the percent inhibition of the SARS-CoV-2 virus. The green squares indicate the percent cytotoxicity of the compounds. Results are representative of n = 6 and are shown as means ± SEMs. EC_{50} and CC_{50} for each compound were calculated by 4-parameter non-linear regression model and were plotted by GraphPad.

Figure 3. Immunofluorescence images of virus infection upon treatment with indicated antivirals. Virus infection and drug treatment were performed as mentioned previously herein. The nuclei (blue) were stained with Hoechst dye. The viral NP protein (green) was stained with rabbit serum against NP, followed by incubation with the secondary antibody, specifically Alexa 488-labeled goat anti-rabbit.

Figure 4. Time-of-drug-addition assay. A, Viral RNA copies in the supernatant were quantified by qRT-PCR; B, NP expression was visualized after arteannuin B treatment at different stages. C, NP expression was quantified by western blot assays after arteannuin B treatment at different stages. D, NP expression was visualized after lumefantrine treatment at different stages. E, NP expression was quantified by western blot assays after lumefantrine treatment at different stages. Results are representative of n = 6 and are means ± SEMs. ***$p<0.001$, significantly different as indicated.

Figure 5. Predictive performance of the drug distribution of lumefantrine. A, The simulated plasma concentration–time profile of lumefantrine following six oral doses of 480 mg over 3 days. A standard population size of 100 individuals was used. The solid line represents the population mean prediction with dashed lines representing the 5th and 95th percentiles of prediction. B,

The predicted lung concentration–time profile of lumefantrine following six oral doses of 480 mg over 3 days. A standard population size of 100 individuals was used. The solid line represents the population mean prediction with dashed lines representing the 5th and 95th percentiles of prediction.

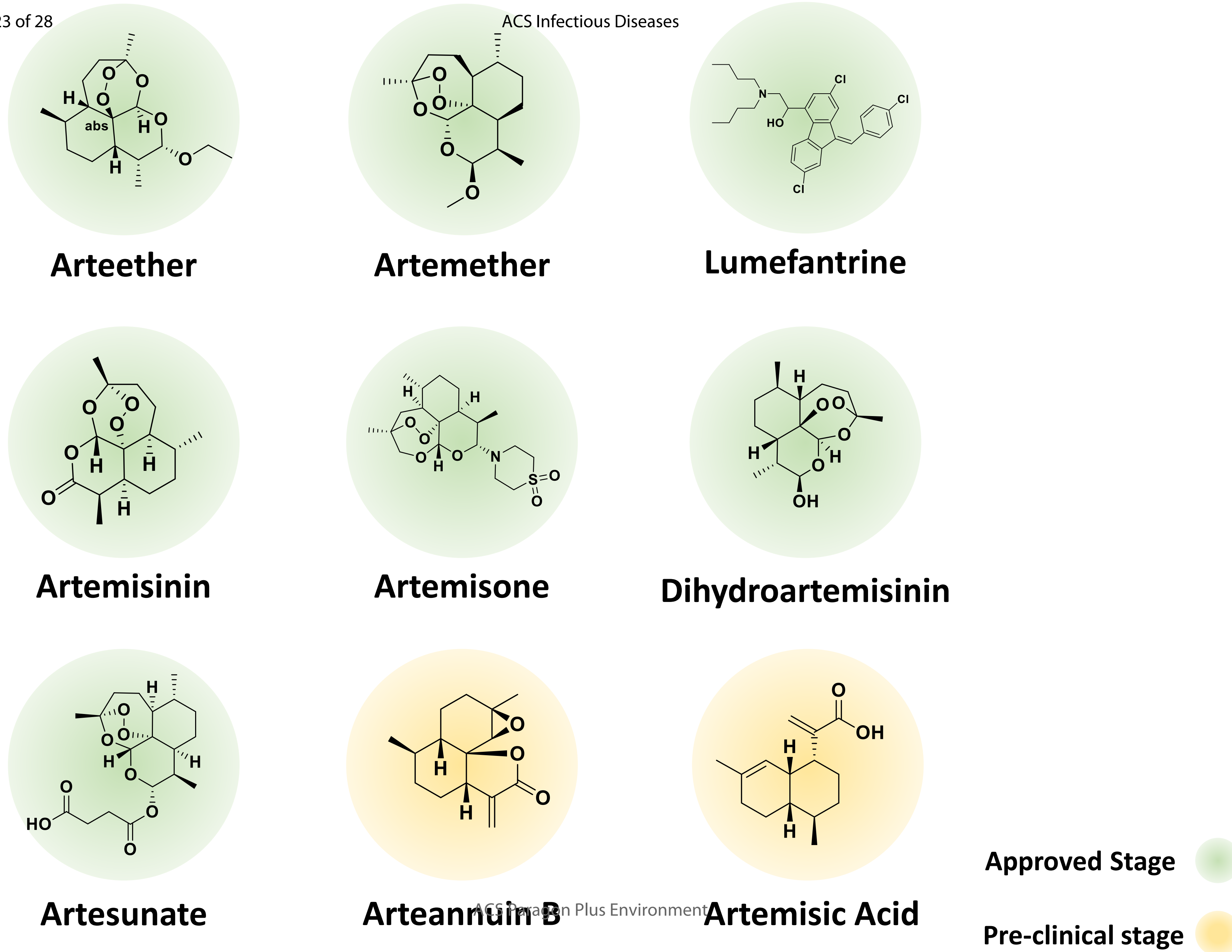
Arteether
Artemether
Lumefantrine
Artemisinin
Artemisone
Dihydroartemisinin
Artesunate
Arteannuin B
Artemisic Acid
Approved Stage
Pre-clinical stage

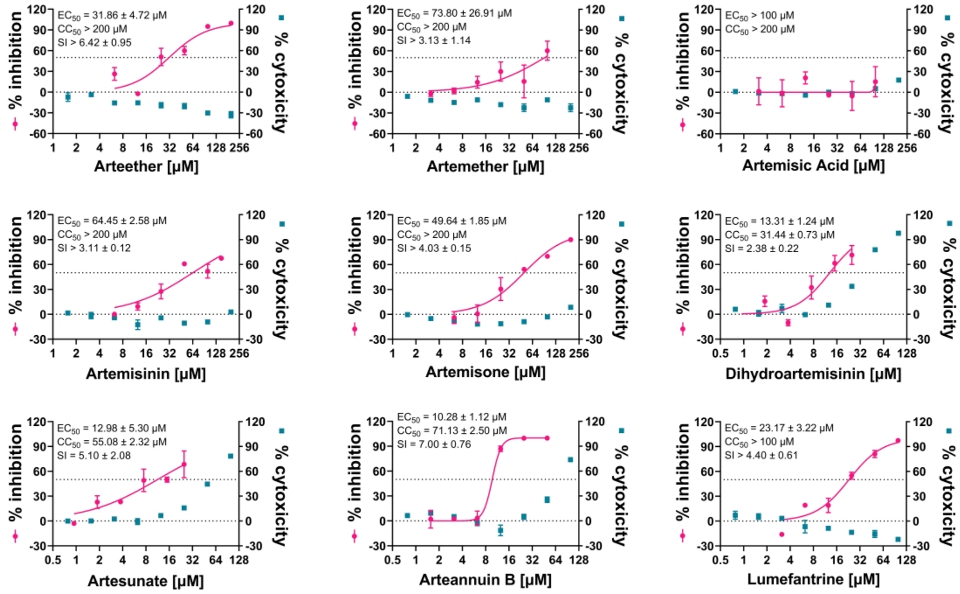

Figure 2. Anti-SARS-CoV-2 profile of selected artemisinins.

164x104mm (1200 x 1200 DPI)

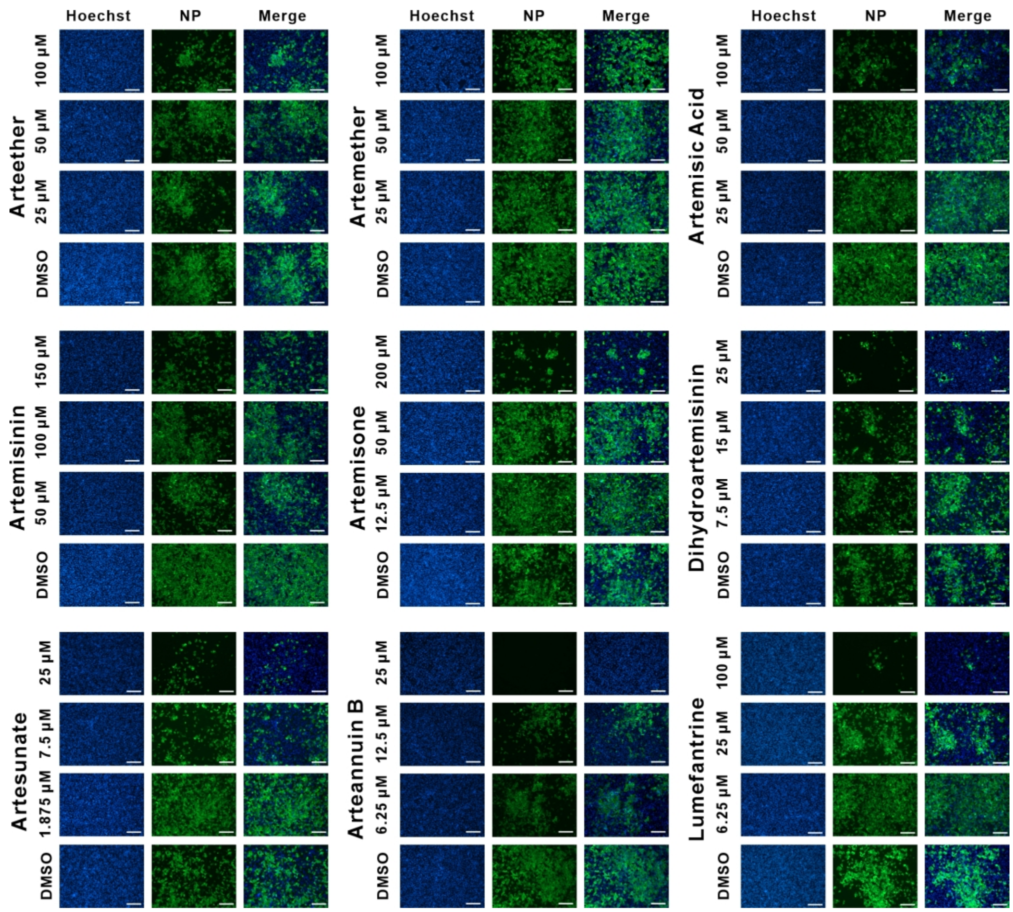

Figure 3. Immunofluorescence microscopy of virus infection upon treatment of indicated antivirals.

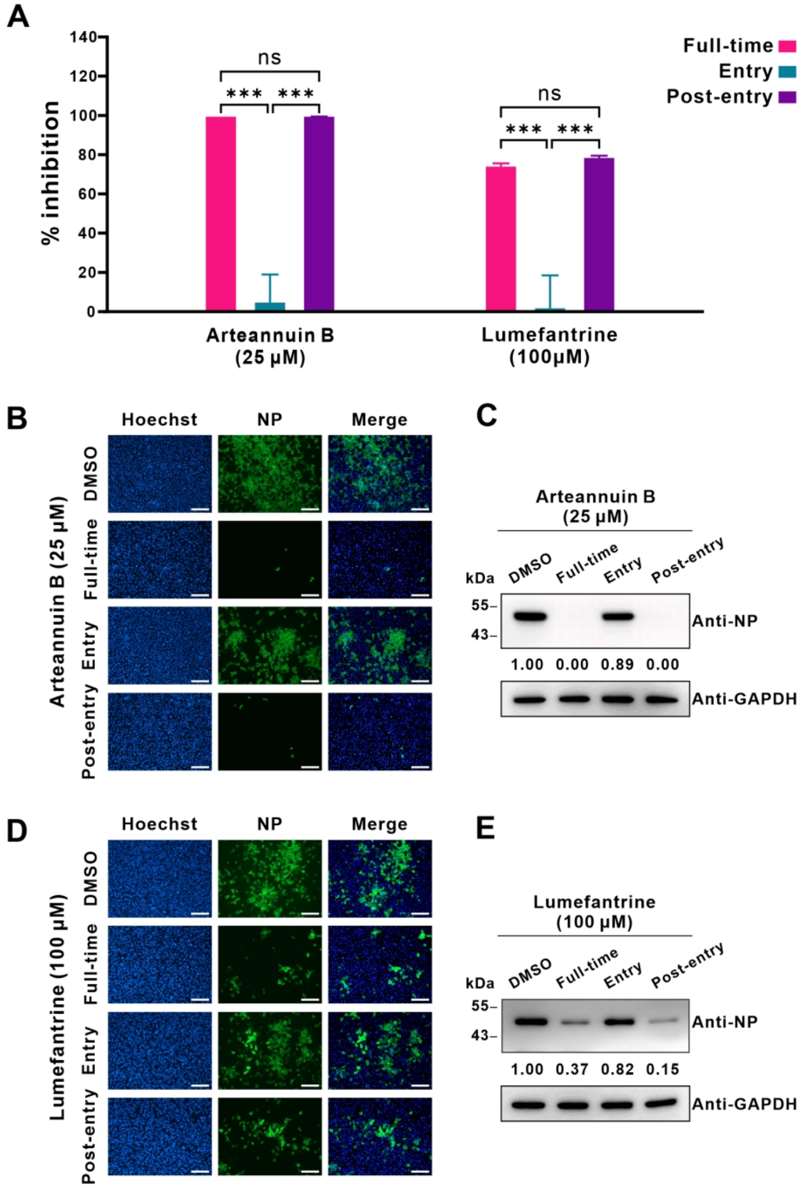

Figure 4. Time of drug addition assay.

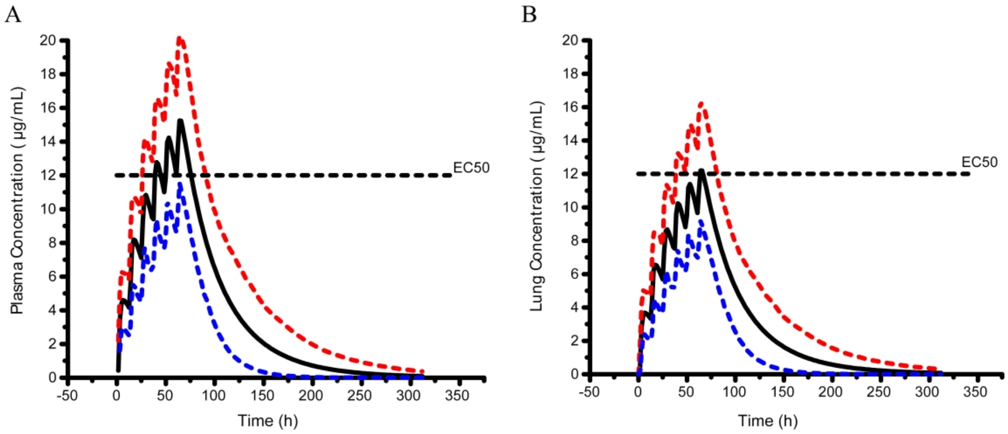

Figure 5. Predictive performance for drug distribution of lumefantrine.

154x66mm (1200 x 1200 DPI)

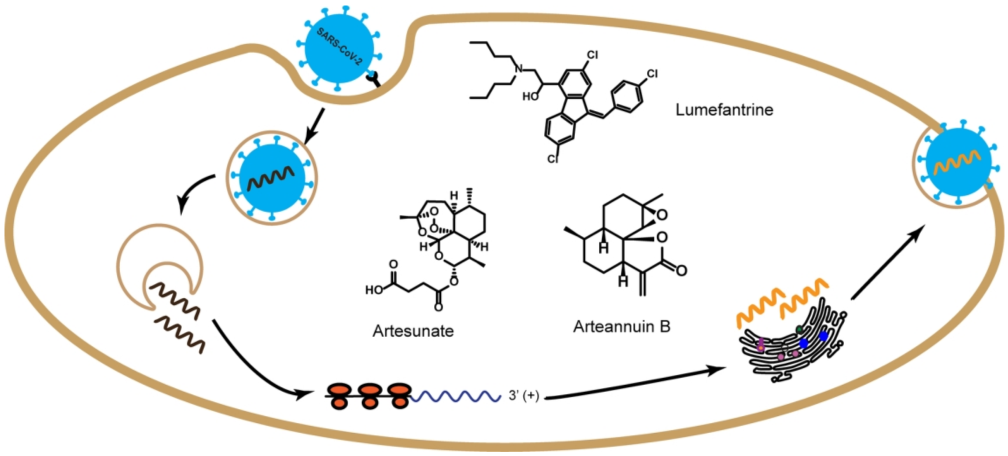

79x35mm (600 x 600 DPI)